A New 2D Zn(II) Coordination Polymer Constructed by Flexible 2-methylimidazole Ligand Exhibiting Good Photocatalytic Degradation of Rhodamine B

Xin-Yue Zhang, Mei-Li Xu, Jun Qing Lv, Xiao-Juan Xu and Jun Wang*
School of Chemistry & Environmental Engineering, Yancheng Teachers University, Yancheng, Jiangsu 224007, P.R. China.
wjyctu@hotmail.com

(Received on 21st Feb 2020, accepted in revised form 14th September 2020)

Summary: A new zinc(II)-coordination polymer, $[Zn(5\text{-}AIP)(BMIOPE)\cdot 2H_2O]_n$ (**1**) (BMIOPE=4,4'-bis (2-methylimidazol-1-yl) diphenyl ether, 5-H_2AIP=5-aminoisophthalic acid) were hydrothermally synthesized. **1** possesses a 2D layer based on opposite-handed helical chains. Furthermore, **1** displays good photocatalytic degradation of Rhodamine B (RhB).

Keywords: Coordination polymer, 2D layer, Flexible imidazole ligand, Photocatalytic degradation.

Introduction

For the recent few decades, how to reassemble coordination polymers (CPs) to have the desired structure is the hot topic in the crystal engineering and material science because of their widely applications in the areas of chemical sensing, magnetism, photo catalysis and so on, not just for their intriguing topological architectures [1–16]. The designing assembly of CPs relies on many factors, including counterions, pH value and solvent system [17–19]. Apart from these external factors, it is worth mentioning that selecting the appropriate organic ligand is also the indispensable factor for the synthesis of CPs. 4,4'-bis(2-methylimidazol-1-yl)diphenyl ether (BMIOPE), which is a flexible V-shaped 2-methylimidazole ligand, can adopt different conformations according to the geometric requirements to multitudinous metal atoms to construct abundant and novel CPs. Furthermore, 5-aminoisophthalic acid (5-H_2AIP) as multidentate O-donor ligands is a prominent building block to build multidimensional dimensional networks with intriguing properties because of their strong coordination abilities and various coordination modes [20–22]. Based on the aforementioned consideration, we selected 5-H_2AIP ligand as the organic carboxylate ligand and simultaneously introduced BMIOPE ligand as the auxiliary ligand to react with Zn(II) ions under solvothermal conditions. Successfully, a novel 2D CP, $[Zn(5\text{-}AIP)(BMIOPE)\cdot 2H_2O]_n$ (**1**) was prepared. The photocatalytic degradation properties of **1** have been discussed.

Experimental

Materials and Physical Measurements

All reagents were purchased from Jinan Trading Company. FT-IR spectra were scanned on an Avatar 360 (Nicolet) spectrophotometer using KBr pellets from 4000 to 400 cm^{-1}. Carbon, hydrogen, and nitrogen elemental analysis were obtained through a Vario EL III elemental analyzer. UV–Vis absorption spectra were carried out by a Cary 500 spectrophotometer.

*Preparation of $[Zn(5\text{-}AIP)(BMIOPE)\cdot 2H_2O]_n$ (**1**)*

$Zn(NO_3)_2\cdot 6H_2O$ (59.4 mg, 0.2 mmol), BMIOPE (33.1 mg, 0.1 mmol), 5-H_2AIP (18.2 mg, 0.1 mmol) were mixed with H_2O (2 mL) and DMF (3 mL), which was placed in a Teflon-lined stainless steel vessel, heated to 100 °C for three days and then cooled to room temperature. Yield: 57.2%. Anal. Calcd for $C_{28}H_{27}N_5O_7Zn$: C, 55.05%; H, 4.45%; N, 11.46%. Found: C, 55.17%; H, 4.46%; N, 11.49%. IR (cm^{-1}): 3577 s, 3402 s, 3111 s, 3066 s, 2966 s, 2878 s, 1678 s, 1604 s, 1508 s, 1343 s, 1250 s, 1162 m, 1012 w, 849 m, 795 m, 738 m, 676 w.

X-ray structure determination

The X-ray diffraction data for **1** were determined on a Bruker SMART APEX II CCD diffractometer equipped with Mo Kα radiation (λ = 0.71073 Å) at 296 K. Absorption correction was performed through the SADABS program [23]. The structure was well solved by direct methods and refined by full-matrix least squares technique through the *SHELXL*-2014 software package [24]. The highly disordered water molecules were deleted through the SQUEEZE program [25]. The crystallographic data are summarized in Table **1**. Table **2** gives selected bond lengths and angles.

*To whom all correspondence should be addressed.

Table-1: Crystal and experimental data of complex **1.**

	1
Empirical formula	$C_{28}H_{27}N_5O_7Zn$
Formula weight	**610.95**
Crystal system	**Monoclinic**
Space group	***P*** $2_1/c$
a **/ Å**	**6.9781(3)**
b **/ Å**	**26.4513(13)**
c **/ Å**	**18.1366(9)**
α **/ °**	**90**
β **/ °**	**101.348(2)**
γ **/ °**	**90**
V **/ Å^3**	**3282.2(3)**
Z	**4**
D_{calc} **/ mg·m^{-3}**	**1.163**
μ(MoK$_\alpha$) / mm^{-1}	**0.787**
F**(000)**	**1184**
Crystal size / mm	**0.21 × 0.20 × 0.19**
Limits of data collection / °	**2.977 ≤ θ ≤ 25.999**
Reflections collected	**169284**
Independent reflections (R_{int})	**6449 (0.0300)**
Data/restraints/parameters	**6449 / 0 / 354**
GOF on F^2	**1.077**
R_1/wR_2 **[I > 2σ(I)]**	**0.0281 / 0.0708**
R_1/wR_2 **(all data)**	**0.0302 / 0.0715**
Largest diff. peak and hole / e·Å^{-3}	**0.226 / -0.317**

$R_1 = \Sigma| |F_o|-|F_c| |/\Sigma|F_o|$. $\omega R_2 = \Sigma[w(F_o^2-F_c^2)^2]/\Sigma[w(F_o^2)^2]^{1/2}$

Table-2: Selected Bond Distances (Å) and Angles (deg) for complex **1.**

Zn(1)-O(1)	**1.9561(12)**	**Zn(1)-N(1)**	**2.0352(14)**
Zn(1)-O(3)#1	**1.9540(11)**	**Zn(1)-N(4)#2**	**2.0428(14)**
O(1)-Zn(1)-N(1)	**118.54(6)**	**O(1)-Zn(1)-O(3)#1**	**107.55(5)**
O(1)-Zn(1)-N(4)#2	**115.25(6)**	**N(1)-Zn(1)-N(4)#2**	**108.82(6)**
O(3)#1-Zn(1)-N(1)	**103.28(5)**	**O(3)#1-Zn(1)-N(4)#2**	**101.21(5)**

Symmetry transformations used to generate equivalent atoms: #1 x, -y+1/2, z+1/2; #2 -x+1, y+1/2, -z+1/2.

Description of the structure

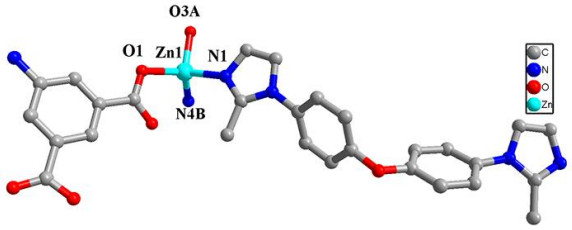

Fig. 1: The coordination environment of Zn(II) in 1. [Symmetry codes: (A): x, -y+1/2, z+1/2; (B): -x+1, y+1/2, -z+1/2].

1 crystallizes in the monoclinic *P* $2_1/c$ space group. There is a Zn atom, a 5-AIP^{2-} ligand, a BMIOPE ligand and two free water molecules in the asymmetric unit of **1**. The Zn1 is surrounded by two carboxylate O atoms (O1 and O3A) from two 5-AIP^{2-} ligands, and two N atoms (N1 and N4B) from two distinct BMIOPE ligands in distorted $\{ZnO_2N_2\}$ tetrahedral geometry with the τ_4 being 0.90 (symmetry code: (A): x, -y+1/2, z+1/2; (B): -x+1, y+1/2, -z+1/2) [26]. The Zn–O distances are 1.9540(11) and 1.9561(12) Å, and the Zn–N distances are 2.0352(14) and 2.0428(14) Å. As shown in Fig. 2, BMIOPE ligands connect neighboring two Zn(II) ions to shape a 1D left-handed $\{[Zn(BMIOPE)]^{2+}\}_n$ single helical chain. In addition, another 1D right-handed $\{[Zn(BMIOPE)]^{2+}\}_n$ single helical chain is also shaped in **1**. Furthermore, these 1D left- and right-handed helical chains are linked by 5-AIP^{2-} ligands to generate a 2D framework (Fig. 3).

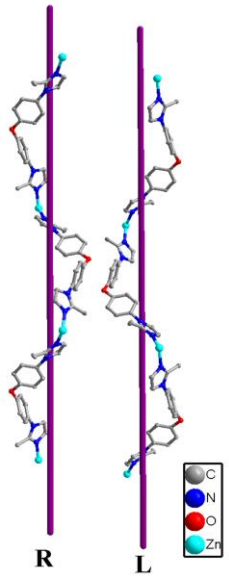

Fig. 2: The (L)-handed and (R)-handed chains constructed by BMIOPE ligands and Zn atoms in **1.**

Photocatalytic properties

Rhodamine B (RhB) was chosen as a model dye to investigate the photocatalytic activity of **1**. 30 mg of **1** and 50 uL of 30% H_2O_2 were dispersed in RhB aqueous solution (50 mL, 10 mg) and then illuminated under a Hg lamp (300 W) with stirring continuously. After intervals of 10 min, RhB aqueous solution (1 mL) was collected, centrifuged and examined by UV-visible spectroscopy. From Figure 4a, the characteristic absorption peak of RhB decreased apparently during the decomposition reaction with the use of **1**. The photocatalytic efficiency on RhB reached 97.1%, and that of the blank control group was only 18.6% within 100 min, indicating **1** have a catalytic activity for the degradation of RhB (Figure 4b).

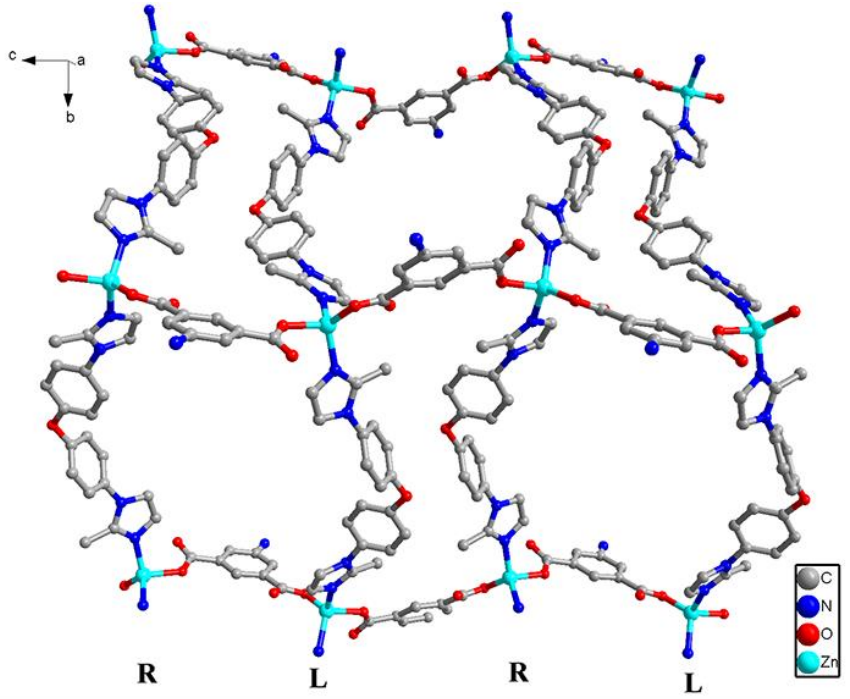

Fig. 3: The 2D layer in **1.**

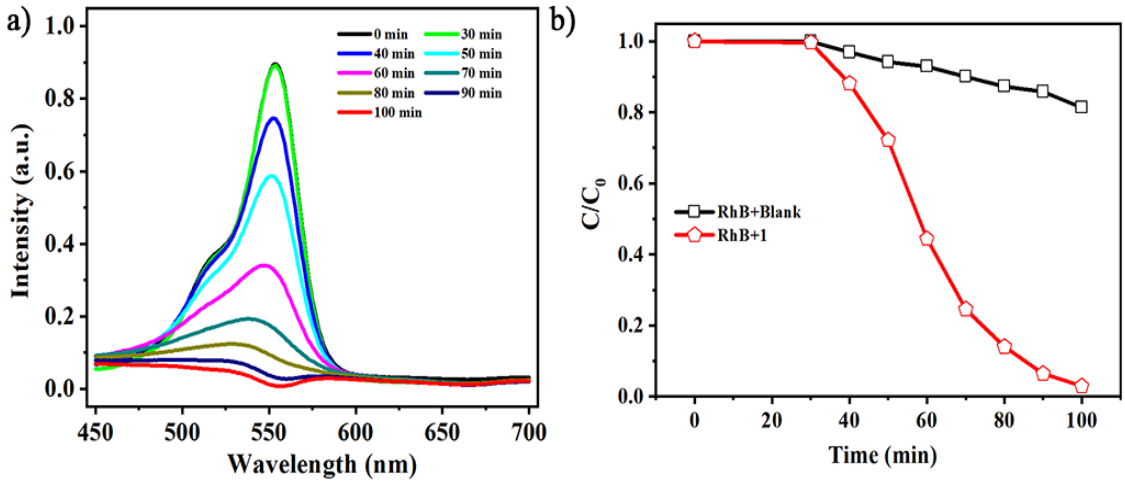

Fig. 4: (a) Absorption spectra of the RhB solution with the use of 1 at different time intervals; (b) Photocatalytic decomposition rate of the RhB solution.

Conclusions

In summary, a new Zn-CP $[Zn(5\text{-}AIP)(BMIOPE)\cdot 2H_2O]_n$ (**1**) was synthesized. **1** is 2D layer based on opposite-handed helical chains. Furthermore, **1** displays good photocatalytic degradation of RhB.

Reference

1 H. Furukawa, N. Ko, Y. B. Go, N. Aratani, S. B. Choi, E. Choi, A. Özgür Yazaydin, R. Q. Snurr, M. O'Keeffe, J. Kim and O. M. Yaghi, Ultrahigh Porosity in Metal-Organic Frameworks, *Science*., **329**, 424 (2010).

2 Y. Cui, Y. Yue, G. Qian and B. Chen, Luminescent Functional Metal–Organic Frameworks, *Chem. Rev*., **112**, 1126 (2012).

3 D. Y. Du, J. S. Qin, S.-L. Li, Z.-M. Su and Y.-Q. Lan, Recent advances in porous polyoxometalate-based metal–organic framework materials, *Chem. Soc. Rev*., **43**, 4615 (2014).

4 J. Y. Zou, W. Shi, H. L. Gao, J.-Z. Cui and P. Cheng, Spin canting and metamagnetism in 3D pillared-layer homospin cobalt(ii) molecular magnetic materials constructed via a mixed ligands approach, *Inorg. Chem. Front*., **1**, 242 (2014).

5 K. J. Gagnon, H. P. Perry and A. Clearfield, Conventional and Unconventional Metal–Organic Frameworks Based on Phosphonate Ligands: MOFs and UMOFs, *Chem. Rev*., **112**, 1034 (2012).

6 M. Zhang, W. Lu, J. R. Li, M. Bosch, Y.-P. Chen, T.-F. Liu, Y. Liu and H.-C. Zhou, Design and synthesis of nucleobase-incorporated metal–organic materials, *Inorg. Chem. Front*., **1**, 159 (2014).

7 S. R. Batten, N. R. Champness, X.-M. Chen, J. Garcia-Martinez, S. Kitagawa, L. Öhrström, M. O'Keeffe, M. Paik Suhh and J. Reedijkij, Coordination polymers, metal–organic frameworks and the need for terminology guidelines, *CrystEngComm*., **14**, 3001 (2014).

8 C. M. Magdalane, K. Kaviyarasu, J. J. Vijaya, B. Siddhardha and B. Jeyaraj, Photocatalytic activity of binary metal oxide nanocomposites of CeO_2/CdO nanospheres: Investigation of optical and antimicrobial activity, *J. Photoch. Photobio. B*., **163**, 77 (2016).

9 C. M. Magdalane, K. Kaviyarasu, J. J. Vijaya, B. Siddhardha and B. Jeyaraj, Facile synthesis of heterostructured cerium oxide/yttrium oxide nanocomposite in UV light induced photocatalytic degradation and catalytic reduction: Synergistic effect of antimicrobial studies, *J. Photoch. Photobio. B*., **173**, 23 (2017).

10 D. Saravanakkumar, H. A. Oualid, Y. Brahmi, A. Ayeshamariam, M. Karunanaithy, A. M. Saleem, K. Kaviyarasu, S. Sivaranjani and M. Jayachandran, Synthesis and characterization of CuO/ZnO/CNTs thin films on copper substrate and its photocatalytic applications, *OpenNano*., **4**, 100025 (2019).

11 N. Geetha, S. Sivaranjani, A. Ayeshamariam, M. S. Bharathy, S. Nivetha, K. Kaviyarasu and M. Jayachandran, High Performance Photo-Catalyst Based on Nanosized ZnO–TiO_2 Nanoplatelets for Removal of RhB Under Visible Light Irradiation, *J. Adv. Res.*, **13**, 12 (2018).

12 S. Himbert, M. Chapman, D. W. Deamer and M. C. Rheinstädter, Organization of nucleotides in different environments and the formation of pre-polymers, *Sci. Rep*., **6**, 1(2016).

13 N. M. I. Alhaji, D. Nathiya, K. Kaviyarasu, M. Meshram and A. Ayeshamariam, A comparative study of structural and photocatalytic mechanism of $AgGaO_2$ nanocomposites for equilibrium and kinetics evaluation of adsorption parameters, *Surf. Interfaces.*, **17**, 100375 (2019).

14 G. T. Anand, D. Renuka, R. Ramesh, L. Anandaraj, S. J. Sundaram, G. Ramalingam, C. M. Magdalane, A. K. H. Bashir, M. Maaza and K. Kaviyarasu, Green synthesis of ZnO nanoparticle using Prunus dulcis (Almond Gum) for antimicrobial and supercapacitor applications, *Surf. Interfaces.*, **17**, 100376 (2019).

15 C. M. Magdalane, K. Kaviyarasu, M. V. Arularasu, K. Kanimozhi and G. Ramalingam, Structural and morphological properties of Co_3O_4 nanostructures: Investigation of low temperature oxidation for photocatalytic application for waste water treatment, *Surf. Interfaces*., **17**, 100369 (2019).

16 Y. Subbareddy, R. N. Kumar, B. K. Sudhakar, K. R. Reddy, S. K. Martha and K. Kaviyarasu, A facile approach of adsorption of acid blue 9 on aluminium silicate-coated Fuller's Earth—Equilibrium and kinetics studies, *Surf. Interfaces*., **19**, 100503 (2020).

17 R.-M. Han, J.-F. Ma, Y.-Y. Liu and J. Yang, Syntheses, structures, and photoluminescent properties of a series of coordination polymers based on a new 2′-carboxybiphenyl-4-ylmethylaminodiacetic acid and different N-donor ligands, *CrystEngComm*., **15**, 5641 (2013).

18 X. Lv, L. Liu, C. Huang, L. Guo, J. Wu, H. How and Y. Fan, Metal–organic frameworks based on the [1,1′:3′,1″-terphenyl]-3,3″,5,5″-tetracarboxylic

acid ligand: syntheses, structures and magnetic properties, *Dalton Trans.*, **43**, 15475 (2014).

19 P. Ramaswamy, N. E. Wong and G. K. H. Shimizu, MOFs as proton conductors–challenges and opportunities, *Chem. Soc. Rev*., **43**, 5913 (2014).

20 Z. Zhou, M.-L. Han, H.-R. Fu, L.-F. Ma, F. Luo and D.-S. Li, Engineering design toward exploring the functional group substitution in 1D channels of Zn–organic frameworks upon nitro explosives and antibiotics detection, *Dalton Trans*., **47**, 5359 (2018).

21 Y. Xiong, G. Liu, X. Wang, J. Zhang, H. Lin and X. Sha, Fluorescent recognition of Fe^{3+} and Fe^{3+}-functionalized composite materials for enhancing photocatalytic activities of Co^{II} complexes, *CrystEngComm*., **19**, 4561 (2017).

22 Y. Wang, P. Xu, Q. Xie, Q.-Q. Ma, Y.-H. Meng, Z.-W. Wang, S. Zhang, X.-J. Zhao, J. Chen and Z.-L. Wang, Cadmium(II)–Triazole Framework as a Luminescent Probe for Ca^{2+} and Cyano Complexes, *Chem-Eur J*., **22**, 10459 (2016).

23 G. M. Sheldrick, *SADABS*, Program for Empirical Adsorption Correction of Area Detector Data, University of Göttingen, Göttingen, Germany, (2003).

24 G. M. Sheldrick, *SHELXL-2014*, Program for the Crystal Structure Solution, University of Göttingen, Göttingen, Germany, (2014).

25 A. L. Spek, *PLATON, A Multipurpose Crystallographic Tool*, Utrecht University: Utrecht, The Netherlands, (2001).

26 L. Yang, D. R. Powell and R. P. Houser, Structural variation in copper(I) complexes with pyridylmethylamide ligands: structural analysis with a new four-coordinate geometry index, τ_4, *Dalton Trans*., **2007**, 955.